REPORT DOCUMENTATION PAGE

Form Approved
OMB No. 0704-0188

1. REPORT DATE *(DD-MM-YYYY)*	2. REPORT TYPE	3. DATES COVERED *(From - To)*
	Technical Papers	

4. TITLE AND SUBTITLE

5a. CONTRACT NUMBER

5b. GRANT NUMBER

5c. PROGRAM ELEMENT NUMBER

6. AUTHOR(S)

5d. PROJECT NUMBER

5e. TASK NUMBER

5f. WORK UNIT NUMBER

7. PERFORMING ORGANIZATION NAME(S) AND ADDRESS(ES)

Air Force Research Laboratory (AFMC)
AFRL/PRS
5 Pollux Drive
Edwards AFB CA 93524-7048

8. PERFORMING ORGANIZATION REPORT

9. SPONSORING / MONITORING AGENCY NAME(S) AND ADDRESS(ES)

Air Force Research Laboratory (AFMC)
AFRL/PRS
5 Pollux Drive
Edwards AFB CA 93524-7048

10. SPONSOR/MONITOR'S ACRONYM(S)

11. SPONSOR/MONITOR'S NUMBER(S)

12. DISTRIBUTION / AVAILABILITY STATEMENT

Approved for public release; distribution unlimited.

13. SUPPLEMENTARY NOTES

14. ABSTRACT

15. SUBJECT TERMS

16. SECURITY CLASSIFICATION OF:			17. LIMITATION OF ABSTRACT	18. NUMBER OF PAGES	19a. NAME OF RESPONSIBLE PERSON
					Leilani Richardson
a. REPORT	b. ABSTRACT	c. THIS PAGE	A		19b. TELEPHONE NUMBER *(include area code)*
Unclassified	Unclassified	Unclassified			(661) 275-5015

9 items enclosed

FILE

MEMORANDUM FOR PRS (In-House Publication)

FROM: PROI (STINFO) 12 July 2002

SUBJECT: Authorization for Release of Technical Information, Control Number: **AFRL-PR-ED-TP-2002-181**
Andrew Ketsdever (PRSA) et al., "Gas Dynamic Calibration of a Nano-Newton Thrust Stand"

56242

Review of Scientific Instruments (Journal) **(Statement A)**
(Deadline: N/A)

Gas Dynamic Calibration of a Nano-Newton Thrust Stand

Andrew J. Jamison[1], Andrew D. Ketsdever[2], E.P. Muntz[1]

[1] Department of Aerospace and Mechanical Engineering
University of Southern California
Los Angeles, CA 90089-1191

[2] Air Force Research Laboratory
Propulsion Directorate
Edwards AFB, CA 93524

Abstract

The ability to measure extremely low thrust levels with unusual precision is becoming more critical as attempts are made to characterize the performance of emerging micropropulsion systems. Many new attitude control concepts for nanospacecraft involve the production of thrust below 1 μN. A simple, but uniquely successful thrust stand has been developed and used to measure thrust levels as low as 86.2 nano-Newtons with an estimated accuracy of ±11%. Thrust levels in the range of 712 nano-Newtons to 1 μN have been measured with an estimated accuracy of ±2%. Thrust is measured from an underexpanded orifice operating in the free molecule flow regime with helium, argon, and nitrogen propellants. The thrust stand is calibrated using results from Direct Simulation Monte Carlo numerical models and analytical solutions for free molecule orifice flow. The accuracy of the gas dynamic calibration technique, using free molecule orifice flow, has also been investigated. It is shown that thrust stand calibration using high Knudsen number helium flow can be accurate to within a few percent in the 80 nN to 1 μN thrust range for thin walled orifices when the stagnation pressure is accurately measured. The thrust stand and calibration technique exhibit significant improvement for accurate, low thrust measurements compared to currently published results.

Nomenclature

A = area
$\vec{c}_o$ = bulk flow velocity
$\overline{c}$ = average thermal velocity
D = damping coefficient
d = diameter
F = force
g = gravitational constant (= 9.81 m/s^2)
I = system inertia
Isp = specific impulse
K = rotational spring constant
k = Boltzmann's constant = 1.38×10^{-23} J/K
Kn = Knudsen number
$\dot{M}$ = mass flow rate
m = molecular mass
n = number density
p = pressure
$\dot{q}$ = heat flux
R = distance from center of rotation to the point of applied force
r = distance from LVDT to center of thrust stand rotation of the nNTS
T = temperature
t = time
$\Im$ = thrust
x = linear deflection
α = transmission probability
λ = mean free path
θ = angular deflection
ω_n = natural frequency

subscripts
fm = free molecule
i = incident
o = stagnation region
r = reflected
t = thruster or orifice
w = wall or plenum

Introduction

The need for thrust measurements below 1μN stems from the development of nano- and pico-spacecraft propulsion systems and missions requiring the precision matching of multiple thrusters. The next generation of nano- and pico-spacecraft will require propulsion systems for constellation formation and maintenance, attitude

control, drag compensation and de-orbit maneuvers. Therefore, thrusters in the micro- and nano-Newton (nN) range will become an ever-increasing part of the aerospace industry. A uniquely successful nano-Newton Thrust Stand (nNTS) has been developed primarily to measure the thrust produced by microelectromechanical systems (MEMS) fabricated propulsion systems such as the Free Molecule Micro-Resistojet (FMMR).[1]

To produce highly repeatable impulse bits on the order of 1 μN-sec, the FMMR will produce a low thrust acting over a relatively long time. Long valve cycle times can improve the accuracy of impulse-bit delivery by minimizing the effects flow unsteadiness associated with valve actuation. To produce an impulse bit of 1 μN-sec, the FMMR will produce a steady state thrust of 100 nN over a 10 second period. Therefore, the continued development of micropropulsion systems will require highly accurate, steady-state measurement techniques in the thrust range between 100 nN and 1 μN. Steady-state thrust measurements as low as 100 nN represent an improvement over state-of-the-art techniques of about 10 times based on currently published results.[2]

Micropropulsion systems capable of producing highly accurate impulse or steady state thrust are required for missions such as the Laser Interferometer Space Antenna (LISA) and the Laser Interplanetary Ranging Experiment (LIRE). Steady state thrust measurements in the range of 1 to 100 μN are required for thruster concepts such as field emission electric propulsion (FEEP) and colloid thrusters. In the case of the LISA mission, FEEP thrusters will be used for attitude control and must have a thrust noise level less than 0.1 μN.[3] The low end of this thrust range coupled with the low noise requirements indicate that thrust stand resolution on the order of 0.01 μN (10 nN) is required for the highly accurate measurements needed for many planned missions.

For larger propulsion systems, it is often necessary to match the performance of two or more thrusters very closely. For example, mission planners might require accurate knowledge of the thrust imbalance of two separate attitude control thrusters for a scientific mission. Also, thruster noise level studies in relatively large-scale propulsion systems may also require thrust stand resolutions in the nano-Newton range. Ultimately,

improvements in thrust stand resolution to 10 nN can have applications to all sizes of spacecraft thruster systems and not just micropropulsion.

Results are presented here from the nNTS for thrust measurements as low as 86 nN. This represents the first time that thrust levels on this order have been accurately measured and reported. A unique calibration technique for thrust measurements below 1 μN is also presented. The calibration utilizes thrust measurements of thin walled, underexpanded orifices in the free molecule flow regime, corrected with results from analytical and Direct Simulation Monte Carlo (DSMC) numerical models.[4] Extremely low, highly accurate thrust measurements are possible with the nNTS because of its unique design and calibration procedures.

Nano-Newton Thrust Stand

Previous investigations into extremely low thrust measurements have been hampered by facility vibrations, thrust stand drift, problems with gas and electrical connections, and calibration concerns. Figure 1 shows the nNTS which was designed to address many of the problems previously experienced in obtaining low thrust measurements. Overall, a design approach was taken that would develop a diagnostic tool that was simple in construction and relatively straightforward in operation. A torsion balance is perhaps the simplest configuration that can be utilized for steady-state or transient thrust measurements. As shown in Fig. 1, two flexure pivots are used to support the thrust stand and provide a restoring force. The pivots have a spring constant of approximately 0.0016 Nm/deg. The nNTS is completely symmetric about the center of rotation with two thrust armatures extending from each side of the stand. The thrust stand arms are approximately 25 cm long from the center of rotation. For thrust measurements below 1 μN, extensions were added to the thrust stand to provide larger deflections for a given thrust as shown schematically in Fig. 2 with the angular deflection, θ, illustrated.

The thrust measurements involve sensing the angular displacement resulting from a torque applied to a damped rotary system. The present method for detecting angular deflection is to measure the linear displacement at a

known radial distance using a Macro Sensors™ linear variable differential transformer (LVDT). The LVDT is an electromagnetic transducer that converts the rectilinear motion of an object into an electrical signal. The LVDT sensor is located approximately 19.7 cm from the center of rotation for the standard configuration and 61 cm from the center of rotation for the extended arm configuration. For a thrust level of 100 nN, the linear movement at the end of the extended configuration's arms is approximately 0.264 μm. Therefore, the error associated with the angular movement of the thrust stand armature is negligible.

As μN and nN thrust levels are approached, the connections of a thrust stand mounted thruster to its supply infrastructure become increasingly difficult to handle. The forces applied by these connections can be orders of magnitude larger than the thrust to be measured. Therefore, the most critical design constraint for nano-Newton thrust measurements comes from not allowing direct mechanical connection of propellant or power feed lines to the thrust stand. This was accomplished in the nNTS through the design of several liquid baths. The purpose of the high viscosity oil bath is shown schematically in Fig. 3. The high viscosity oil serves two purposes for thrust stand operation. First, the oil acts as a gas seal whereby propellant fed into the inverted cylinder of the thrust stand can not escape into the surrounding vacuum except through the propulsion system. Liquid seals for gas containment have been investigated in previous research.[5] With this configuration, propellant feed lines are not directly connected to the thrust stand. The propellant introduced into the thrust stand's inverted cylinder moves into the cylindrical arms of the thrust stand and subsequently into the thruster's stagnation chamber. Second, the oil acts as a viscous damper for the thrust stand system. The level of viscous damping of the thrust stand can be changed by varying the height of the oil on the sides of the inverted cylinder. Great care was taken to identify an appropriate oil with high viscosity, low vapor pressure and negligible solubility for propellants of interest. The Dow Corning oil used has a viscosity of 10,000 C.S. and a specific gravity of 971 kg/m^3.[6]

Analysis

Thrust Stand Dynamics

The thrust stand is a torsion balance with the oil bath acting as the viscous damper of the system. The system can be characterized by a second order differential equation that accounts for the various moment contributions.[7]

$$I\ddot{\theta} + D\dot{\theta} + K\theta = FR \tag{1}$$

For a rotational system as in the case of the nNTS, the spring constant K is in units of Nm/rad. The solution for the angular deflection of the nNTS can be derived as a function of time. For a steady-state thrust, F, the deflection is given as

$$\theta(t) = \frac{FR}{K} + \frac{FR}{K} e^{-bt} \sin(\omega_n t) \tag{2}$$

where

$$b = \frac{D}{2I} \tag{3}$$

and the natural frequency, ω_n, is

$$\omega_n = \sqrt{\frac{K}{I} - b^2} \tag{4}$$

The angular deflection of the thrust stand for the steady-state condition is

$$\Delta\theta = \frac{FR}{K} \tag{5}$$

Figure 4 shows a theoretical nNTS trace with a steady-state applied force from Eq. (2). The initial deflection is nearly twice that of the steady-state condition, but the damping quickly reduces the oscillations to the steady-state thrust level from Eq. (5). Solutions to the equation of motion for torsional thrust stands with a transient impulse have been presented elsewhere and agree with the above formulation for steady-state thrust.[8, 9]

Underexpanded Free Jets

As previously mentioned, the thrust stand uses underexpanded orifices operating in the free molecule flow regime for calibration. For free molecule flow, the Knudsen number defined by

$$Kn_t = \frac{\lambda_o}{d_t} \tag{6}$$

is relatively high (Kn ≥ 10). This is realized at very low stagnation pressures where the molecular mean free path is much larger than the orifice diameter. The free molecule mass flow and thrust are given by

$$\dot{M}_{fm} = \alpha m \frac{n_o \overline{c}}{4} A_t = \alpha m n_o \frac{\sqrt{\frac{8kT_o}{\pi m}}}{4} A_t \tag{7}$$

$$\Im_{fm} = \alpha \frac{p_o}{2} A_t \tag{8}$$

To use Eq. (8) for thrust stand calibration, errors associated with the transmission probability, the measurement of the orifice area, and the measurement of the stagnation pressure must be taken into account. For simple calibration of the nNTS, the use of Eq. (8) is desired; however, its accuracy must be validated in the thrust range of interest. It is expected that the form of Eq. (8) will only be reasonably accurate for free molecule flows since this assumption was used in its derivation. The applicability and accuracy of the analytical thrust equation for free molecule flow through an orifice will be determined through comparison with DSMC results.

A simple analytical expression for the free molecule transmission probability can be derived for t « d_t which yields

$$\alpha = 1 - \frac{2t}{d_t} \tag{9}$$

The transmission probability is defined as the ratio of gas molecules which enter the finite thickness orifice to those that exit. The finite thickness correction assumes fully diffuse wall collisions and neglects multiple orifice wall interactions. For thin walled orifices, the transmission probability α should be very close to unity.[10] The thickness to diameter ratio for the orifice used in this study was t/d = 0.015 which gives $\alpha = 0.97$.

Experimental Set Up and Procedure

The nNTS was installed in Chamber-IV of the Collaborative High Altitude Flow Facility (CHAFF-IV) at the University of Southern California. CHAFF-IV is a 3 m diameter by 6 m long stainless steel vacuum chamber shown schematically in Fig. 5. Although CHAFF-IV is a cryogenically pumped, space simulation facility,[11] only a single diffusion pump was used for the reported experiments. The Zyrianka 900 diffusion pump has an ultimate pumping speed of 25,000 L/sec for nitrogen and 42,000 L/sec for helium. The ultimate facility pressure in CHAFF-IV is approximately 1.0×10^{-6} Torr with the single diffusion pump operating. The 1.0 m diameter diffusion pump is backed with a 2000 L/sec Roots blower system. The location of the thrust stand in CHAFF-IV relative to the pumping system and background gas inlet is also shown in Fig. 5. The background gas inlet was used to investigate the effects of facility background pressure on the thrust measurements. During experiments in CHAFF-IV, the background pressure varied from 10^{-6} to 10^{-5} Torr over the range of operational orifice stagnation pressures.

An underexpanded orifice was tested due to the simplified geometry and flow characteristics as compared to other candidate propulsion systems, although the thrust stand was designed to support several complex micropropulsion devices. The orifices were conventionally machined in a tantalum shim with a diameter of 1 mm ±0.025 mm and

a wall thickness of 0.015 mm (t/d ≐ 0.015). The orifices were attached to aluminum plenums as shown in Fig. 6 with thrust vectors in opposite directions for increased deflection of the armatures. Nitrogen, helium, and argon were used as cold gas propellants (T_0 = 297 K) at various stagnation pressures.

Pressure is measured, both in the nNTS's inverted cylinder and in the stagnation chamber of the orifice, with MKS™ 0.2 Torr pressure transducers. The propellant is introduced into the stagnation chamber of a thruster through an adjustable needle valve located downstream of a thermal, flow through mass flow meter. In the experimental configuration, the mass flow meter operated in the continuum regime throughout the pressure range studied. Thrust measurements were obtained using the underexpanded orifice over the range of stagnation pressures from 8×10^{-4} to 1×10^{-2} Torr. Data for stagnation pressures in this range were taken with the nNTS using the extended armatures as shown in Fig. 2.

The signal from the thrust stand LVDT was sent to a 24-bit digitizing card installed in a PC. Since the digitizer voltage range was from –7.5 to +7.5 V, the associated bit noise from the digitizer is approximately 0.894 μV. The LVDT had a sensitivity of 260 mV/mm implying that the data acquisition system is limited to deflections several times greater than 3.4×10^{-3} μm. Figure 7 shows the bit noise from the data acquisition system without connection to the thrust stand LVDT and with connection to the LVDT. The top data trace in Fig. 7 represents the level of system noise external to the thrust stand system. The bottom data trace in Fig. 7 shows the digitizer signal with the LVDT connected to the thrust stand showing the zero-thrust noise environment experienced in CHAFF-IV. As indicated by the comparison of the data traces in Fig. 7 the noise environment experienced by the nNTS in CHAFF-IV is only slightly larger than the inherent noise of the detection system.

Results

The thrust stand deflection for argon, nitrogen, and helium propellants are shown in Fig. 8 as a function of the stagnation pressure over the range of p_o = 0.8 to 10 mTorr. Each data point in Fig. 8 represents the average of at

least 5 individual test runs at a given stagnation pressure. The error in Fig. 8 is the $\pm \sigma$ error for all the tests at a given stagnation pressure, which represents the error in the repeatability of the nNTS deflection measurement. Errors in the deflection measurement arise from errors in accurately measuring the stagnation pressure, thrust stand drift, and other anomalies in the thrust stand operation.

The Knudsen number ranges from approximately 20 to 167 for the helium flow in the pressure range shown in Fig. 8. Over this range, the flow can be considered free molecular, and the trend in the deflection (or thrust) versus stagnation pressure is expected to be linear as Eq. (8) indicates. As long as the flow satisfies the free molecule conditions, Eq. (8) is independent of the propellant gas. Therefore at large Kn, different propellants at the same stagnation pressure should produce the same free molecule thrust assuming that internal energy effects are negligible. The mean free paths for nitrogen and argon are approximately a factor of three lower for a given stagnation pressure than for helium, indicating that the analytical solution for the thrust from Eq. (8) is only valid for stagnation pressures less than 5×10^{-3} Torr (i.e. where $Kn \geq 10$). In all cases it was assumed that the gas temperature was within $\pm$ 1 K of the local ambient temperature (297 K), as established by thermocouple measurements in separate tests of an operating orifice.

For nitrogen and argon, the Knudsen number ranges from approximately 5 to 56 in the pressure range shown in Fig. 8. Because of the relatively high Kn, it is expected that the deflection versus stagnation pressure for these free molecule flows should be nearly the same. The nitrogen free molecule thrust appears to be slightly higher than that for helium and argon at the same stagnation pressure which may indicate that internal energy is being added to the flow through rotation-translation collisional exchange.

Figure 9 shows a typical trace from the nNTS LVDT for a stagnation pressure of 7 mTorr. For Fig. 9(a), the armature was extended on only one side of the thrust stand with no mass balancing on the opposite side. For Fig. 9(b), both sides of the nNTS were extended in an attempt to mass balance the stand. Both traces are for nitrogen

gas at the same thrust level. The environmental noise in the data was reduced by a factor of 10 for the symmetric thrust stand configuration indicating the importance of mass balancing the stand for thrust measurements in the nano-Newton range.

Calibration

The calibration of the nNTS for steady-state thrusts is complicated by the very nature of the extremely small forces being measured. Conventional methods of calibration such as hanging weights from an armature with a string/pulley system were attempted with little success. Typically small errors associated with the weight calibration scheme such as friction in the pulley/string system become increasingly important in the range of thrust below 1 μN. For the accurate steady-state calibration of the nNTS below 1 μN, a new technique was required.

The DSMC numerical model was used to obtain the thrust for the underexpanded orifice operating in the free molecule flow regime.[12] The DSMC simulations used experimentally determined stagnation pressures, temperatures, and mass flows as boundary conditions. Table 1 shows the DSMC and analytically derived thrust from Eq. (8) for helium flow with Knudsen numbers greater than 20. Because the DSMC solutions were obtained for an infinitely thin orifice, a calibration correction was determined for the finite orifice thickness used in the experiment. A transmission probability for the thin walled orifice used in this study is approximately $\alpha = 0.97$ which was used to obtain the values in Table 1. The DSMC technique has been extensively validated in other studies[4] and is a widely accepted numerical approach for rarefied flows.

As indicated in Table 1, the thrust derived from the DSMC method and the analytical equation (Eq. (8)) are within 1.2% over the investigated range of thrust. The helium experimental results from Fig. 8 and the numerical results in Table 1 are used to generate the calibration plot in Fig. 10. As expected, the thrust stand deflection versus orifice thrust has a linear dependence. The linear calibration is found by the least-squared method for the helium

data at high Knudsen numbers where the DSMC and analytical solutions are expected to be highly accurate. Different schemes and procedures were used to generate the calibration line; however, the error associated with these different procedures was found to be less than 1%.

The thrust generated by the orifice at high Knudsen number should be independent of the gas used for a given stagnation pressure, assuming that internal energy modes do not affect the thrust significantly. Figure 11 shows the same calibration line shown in Fig. 10 plotted against the data for nitrogen and argon gases. As expected, the calibration line fits the nitrogen and argon data quite well. Figure 12 is used as a check on the applicability of the calibration factor for the orifice flow at high Knudsen number.

For future nNTS calibration, the use of the analytical thrust equation (Eq. (8)) is valid assuming the calibration orifice is operated at high Knudsen number. Since internal energy modes can create errors in the thrust determined by Eq. (8), monatomic gases such as helium and argon should be used for calibration. Future thrust stand operation will utilize an underexpanded orifice on one armature to provide in-situ calibration of the stand when propulsion systems are being tested on the other armature as shown schematically in Fig. 3.

Discussion

Possible Errors in the Gas Dynamic Calibration

Analysis was performed to assess errors generated by assumptions in the gas dynamic calibration. For example, the orifice plenum surface temperature was measured in vacuum as T_w = 297K with a typical helium gas flow. An assumption was made that the gas temperature was fully accommodated to the plenum temperature such that $T_o = T_w$. The average number of wall collisions between a typical gas molecule and the plenum walls is approximated by the ratio of the plenum area to the orifice area. For the geometry used in this study, the average number of wall collisions for a gas molecule in the plenum is about 780 before expanding through the orifice into the vacuum system. Using the definition of the accommodation coefficient, an expression can be derived for the ratio of the reflected energy flux from a wall to the energy flux from the wall assuming full accommodation.

$$\left(\frac{\dot{q}_r}{\dot{q}_w}\right)_j = \frac{1}{2}\left\{\left(\frac{\dot{q}_i}{\dot{q}_w}\right)+1\right\} \tag{10}$$

where j is the wall collision number, $\dot{q}_r$ is the reflected heat flux from the wall, $\dot{q}_i$ is the incident heat flux to the wall, $\dot{q}_w$ is the heat flux from the wall assuming full accommodation. For collision j, $\dot{q}_i = (\dot{q}_r)_{j-1}$. Assuming a worst case accommodation coefficient of 0.5 and a gas inlet temperature to the plenum of 150 K, the gas molecule will have a temperature of 0.999 T_w after 9 wall collisions. Therefore, the expected error due to unknown gas temperature is expected to be negligible since the molecules will experience 780 wall collisions on average.

Another error associated with the calibration technique is the effect of the gas bulk flow or drift velocity. The analytical expressions for the thrust and mass flow in Eqs. (7) and (8) assume that the only component of the molecular velocity across the orifice exit plane is thermal. This is fundamentally correct for the large fraction of molecules that have several wall collisions before expanding through the orifice since the thermal accommodation to the plenum walls would effectively remove any bulk flow dependence. However, some fraction of the molecules entering the plenum may escape directly through the orifice without wall collisions. As a worst case analysis, the mass flow into the plenum is assumed to be traveling at a bulk flow velocity $\vec{c}_o$. The bulk flow velocity would transport molecules with a direct line of site to the orifice as they entered the plenum. The direct line of site transport constitutes an error in the thrust calculated in Eq. (8) which assumes only thermal velocity transport of molecules through the orifice. The solid angle for bulk flow transport through the orifice to occur is relatively small since the plenum area is relatively large compared to the orifice area, and the plenum inlet is perpendicular to the orifice exit plane. For the plenum and orifice geometry in this study, the bulk flow velocity would lead to less than a 0.36% error in calculated thrust obtained by Eq. (8). Since the magnitudes of the worst-case errors associated with the gas temperature and bulk flow velocity are very small, they are neglected as sources of error for the gas dynamic calibration technique.

Error Analysis

For free molecule flow, the solutions obtained by the DSMC and analytical approaches are expected to be highly accurate. Sensitivity studies were performed with the DSMC to insure the solution was independent of grid spacing and number of simulated molecules.[12] Therefore the error in thrust calibrations is approximately ±10.6% at the lowest helium thrust level due primarily to errors in measuring the stagnation pressure, the orifice diameter, and assuming a transmission probability of unity. The experimentally derived stagnation pressures, temperatures, and orifice diameter were used in the DSMC and analytical calculations as known parameters.

At the lowest helium stagnation pressure, $p_o = 8.5 \times 10^{-4}$ Torr, the error in the deflection calculated from the standard deviation is ±9.5%. At $p_o = 6.93 \times 10^{-3}$ Torr, the standard deviation in the deflection data is ±1.1%. Experimental error in measuring the thrust stand deflection comes from a variety of sources including errors in stagnation pressure measurement, system noise, and thrust stand drift. Although to some extent all of the sources of error are contained in the standard deviations quoted above, attempts were made to correct the measured deflection for the measured nNTS drift rate. The thrust stand drift rate was observed to be relatively constant over a particular steady-state thrust measurement, which allowed for straightforward correction. An example of the nNTS drift over a 5 minute steady-state thrust measurement can be seen in Fig. 9. At the indicated 712 nN thrust level, the drift was found to be less than 2% of the measured deflection. At 86.2 nN, the drift was approximately 15% of the measured deflection over a 5 minute measurement. Because the drift rate was relatively constant throughout the operation of the nNTS, any errors associated with the drift were able to be corrected in the final data analysis (e.g. Figures 10 and 11).

Errors associated with adsorption and emission of molecules from thruster surfaces or from the damping oil reservoir have been found to be negligible. The use of helium as the calibration gas minimizes adsorption on thruster surfaces. Long-term helium flow also does not show measurable adsorption into the viscous oil used for damping the nNTS.

Table 2 shows the associated error in the thrust measurement expected at the two extremes of the data collected in this experimental study. For the helium data, the calibration from Table 1 and the error from Table 2 indicates that the lowest stagnation pressure $p_o = 8.5 \times 10^{-4}$ Torr produces a thrust of 86.2 nN ±10.7%. At $p_o = 6.93 \times 10^{-3}$ Torr, the thrust is 712 nN ±2%. Most of the error in the determination of the orifice produced thrust at low stagnation pressure comes from uncertainties in the pressure measurement and the scatter in the deflection data.

Facility Effects

It is known that the deflection for a given orifice stagnation pressure is dependent on the background pressure of the facility.[13] Figure 12 shows the measured deflection for nitrogen as a function of facility background pressure for several stagnation pressures. As seen in Fig. 12, the measured thrust tends towards the asymptotic limit at lower facility background pressures. For the range of stagnation pressures investigated in this study, the facility background pressure remained below 1×10^{-5} Torr. Therefore, the error in the thrust measurements associated with the facility background are assumed to be negligible.

Gas Dynamic Calibration Technique: Design Criteria and Issues

Several issues in the design of the free molecule orifice and plenum configuration must be considered to ensure that the gas dynamic calibration technique can be applied with minimal departure from the analytical model. To reduce the effects of having an unknown gas temperature and bulk flow contribution to the thrust, the plenum to orifice area ratio must be very large. A large area ratio will result in the gas becoming essentially fully accommodated to the temperature of the plenum walls, making the effects of having an unknown gas temperature negligible while removing the bulk flow velocity component from the majority of the gas molecules. To further reduce the bulk flow contribution, placing the orifice exit plane perpendicular to the gas inlet reduces the solid angle through which gas entering the plenum could escape directly through the orifice with no wall collisions.

In addition the analytical model does not take into account an orifice with a finite thickness. To minimize the reduction in thrust due to gas molecule collisions with the orifice walls, the thickness to diameter ratio must be very small.

Acknowledgements

The authors are grateful to Prof. Deborah Levin and Ms. Alina Alexeenko (The Pennsylvania State University) for providing the DSMC calibration results. This work was supported by the Air Force Research Laboratory's Propulsion Directorate (AFRL/PRSA).

References

1. A.D. Ketsdever, et al., "Predicted Performance and Systems Analysis of the Free Molecule Micro-Resistojet," *Micropropulsion for Small Spacecraft*, Progress in Astronautics and Aeronautics, , edited by M. Micci and A. Ketsdever, Vol. 187, pp. 167-183 (AIAA, Reston, VA, 2000).

2. L. Boccaletto and L. d'Agostino, "Design and Testing of a Micro-Newton Thrust Stand for FEEP," AIAA paper No. 2000-3268, July, 2000.

3. W. Folker, et al., "LISA Mission Concept Study," Jet Propulsion Laboratory Publication 97-16, March 1998.

4. G.A. Bird, *Molecular Gas Dynamics and the Direct Simulation of Gas Flows*, (Clarendon Press, Oxford, England, 1994).

5. E.P. Muntz, "Pressure Measurements in Free Molecule Flow with a Rotating Arm Apparatus," UTIA TN 22, 1958.

6. E. J. Beiting, "Impulse Thrust Stand for MEMS Propulsion Systems," AIAA paper No. 99-2720, June 1999.

7. E. Doebelin, *Measurement Systems: Application and Design*, (McGraw-Hill, New York, 1966).

8. T.W. Haag,, Rev. Sci. Instrum., 68, 2060 (1997).

9. E.A. Cubbin, et al., Rev. Sci. Instrum., **68**, 2339 (1997).

10. J. Lafferty, *Foundations of Vacuum Science and Technology*, (John Wiley and Sons, New York, 1998).

11. A.D. Ketsdever, J. Spacecr. Rockets, **38**, 400 (2001).

12. A.A. Alexeenko, A.A., et al., "Numerical and Experimental Study of Orifice Flow in the Transitional Regime," AIAA paper No. 2001-3072, June, 2001.

13. A.D. Ketsdever, A., J. Prop. Power, accepted for publication.

P_o (mTorr)	K_n	$\Im$ (nN) (DSMC)	$\Im$ (nN) (analytical)
0.85	167.1	86.2	86.3
1.38	102.9	140.7	140.1
2.05	69.3	209.7	208.2
3.39	41.9	347.6	344.3
5.15	27.6	528.8	522.9
6.93	20.5	712.1	703.7

Table 1: Free molecule calibration data for helium.

$\Im$ (nN)	DSMC Calibration Error		Experimental Error	
	Error in α	Error in d_t (mm)	Deflection $\pm \sigma_D$ (%)	Thrust $\pm \sigma_\Im$ (%)
86.2	0.97 ± 0.003	1 ± 0.025	9.5	10.7
712.1	0.97 ± 0.003	1 ± 0.025	1.1	2.0

Table 2: Errors contributing to the thrust error.

Figure Captions

Figure 1: The nano-Newton Thrust Stand (nNTS) installed in a vacuum chamber.

Figure 2: The nNTS with extended armatures.

Figure 3: Schematic of thrust stand oil bath acting as propellant seal and viscous damper.

Figure 4: Deflection of a damped system with a constant thrust.

Figure 5: CHAFF-IV schematic with thrust stand location.

Figure 6: Orifice geometry.

Figure 7: Bit noise from data system and environmental noise from the LVDT connected to the nNTS.

Figure 8: Deflection as a function of stagnation pressure for nitrogen, helium, and argon.

Figure 9: a) Thrust stand trace for nitrogen with P_0=.007 Torr with one arm extension. b) Thrust stand trace for nitrogen with P_0=.007 Torr with both arm extensions.

Figure 10: Calibration line derived from DSMC thrust versus experimental deflection for free molecule helium flow.

Figure 11: Calibration line with analytically derived thrust versus experimental deflection for nitrogen and argon.

Figure 12: Normalized deflection versus CHAFF-IV background pressure for nitrogen flow at various stagnation pressures.

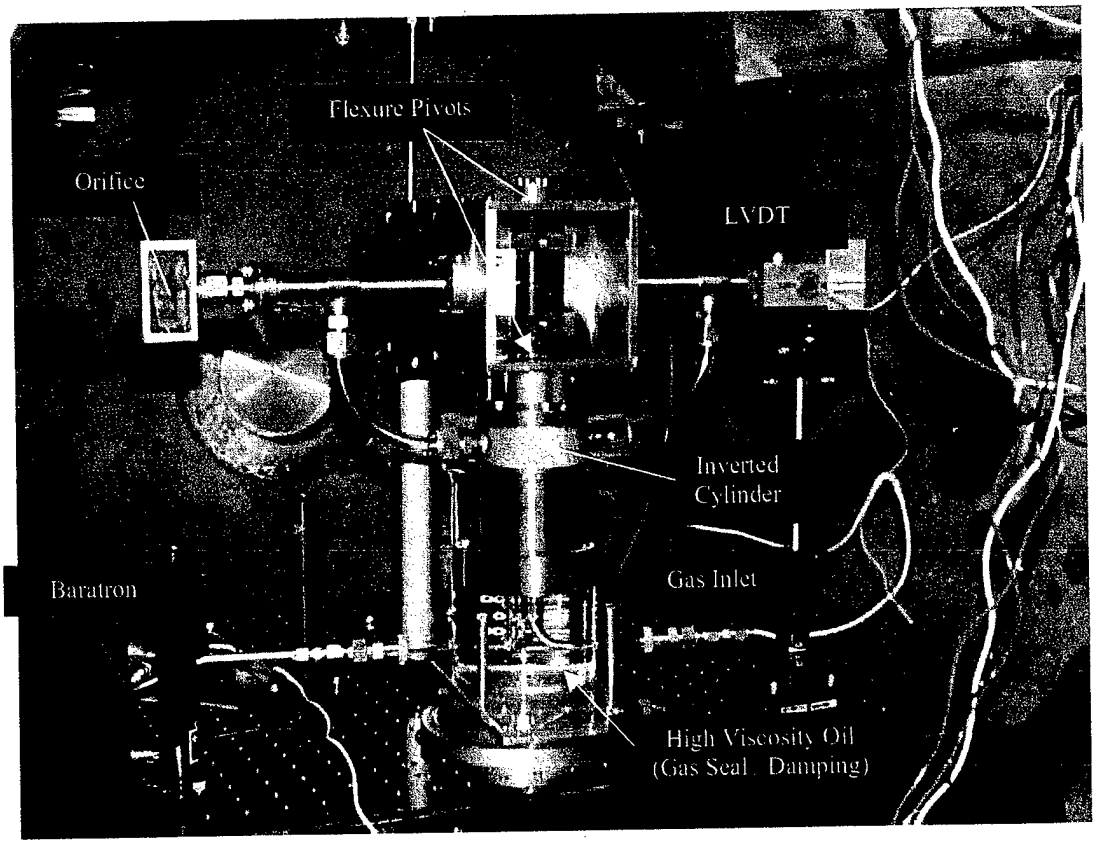

Figure 1 Jamison

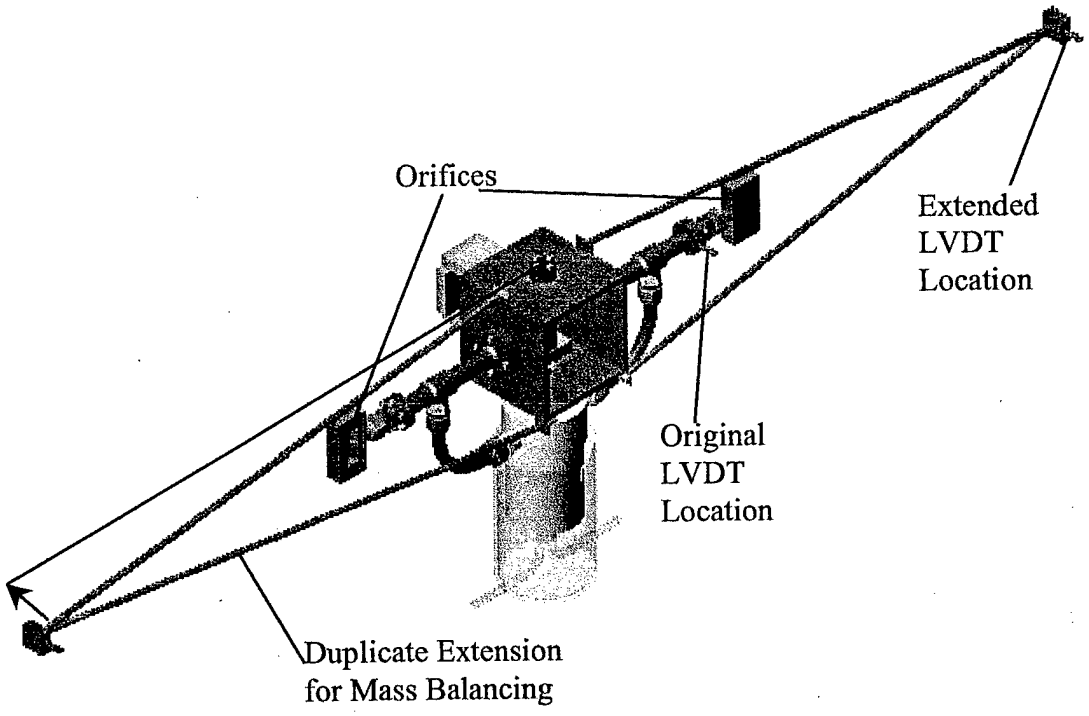

Figure 2 Jamison

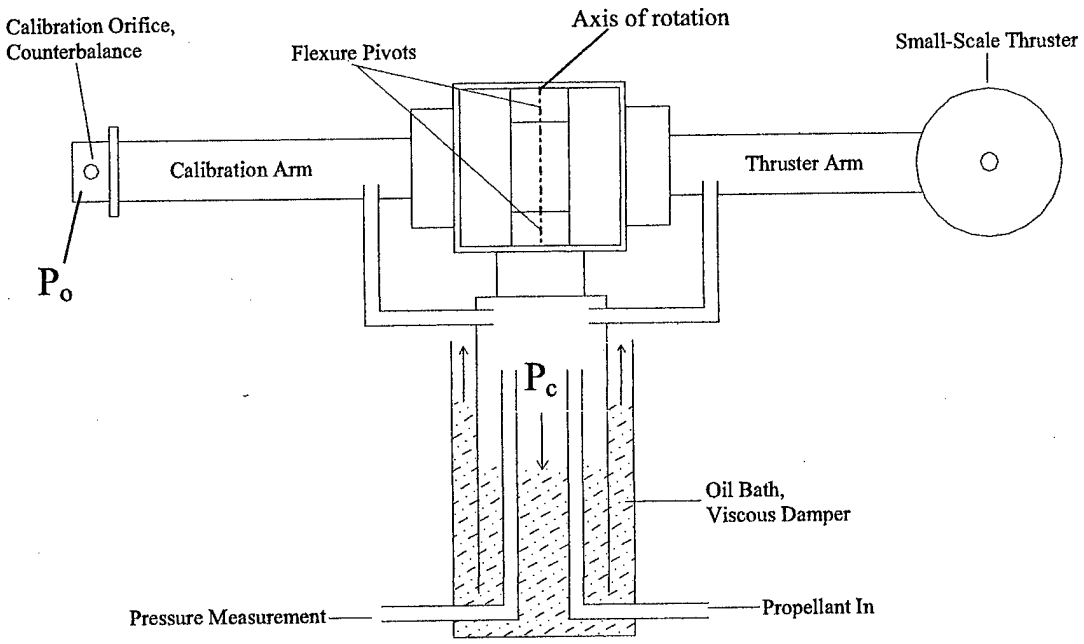

Figure 3 Jamison

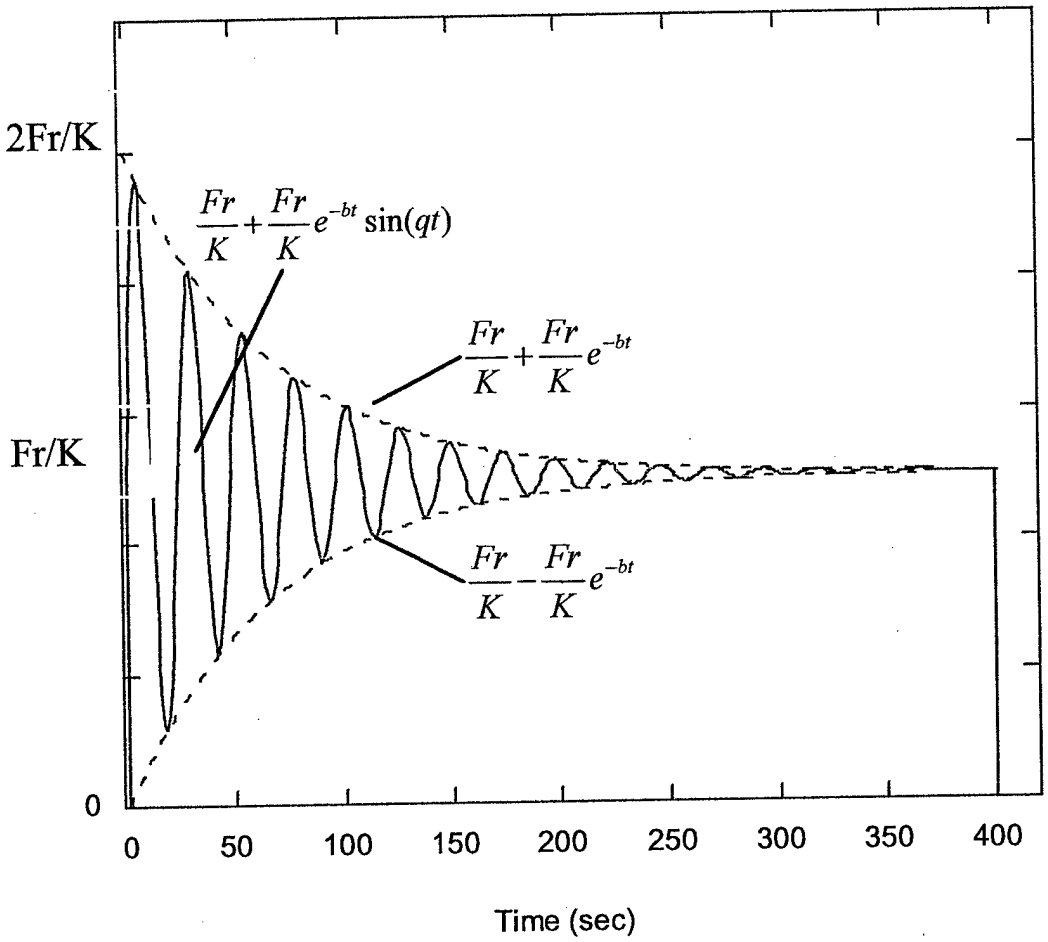

Figure 4 Jamison

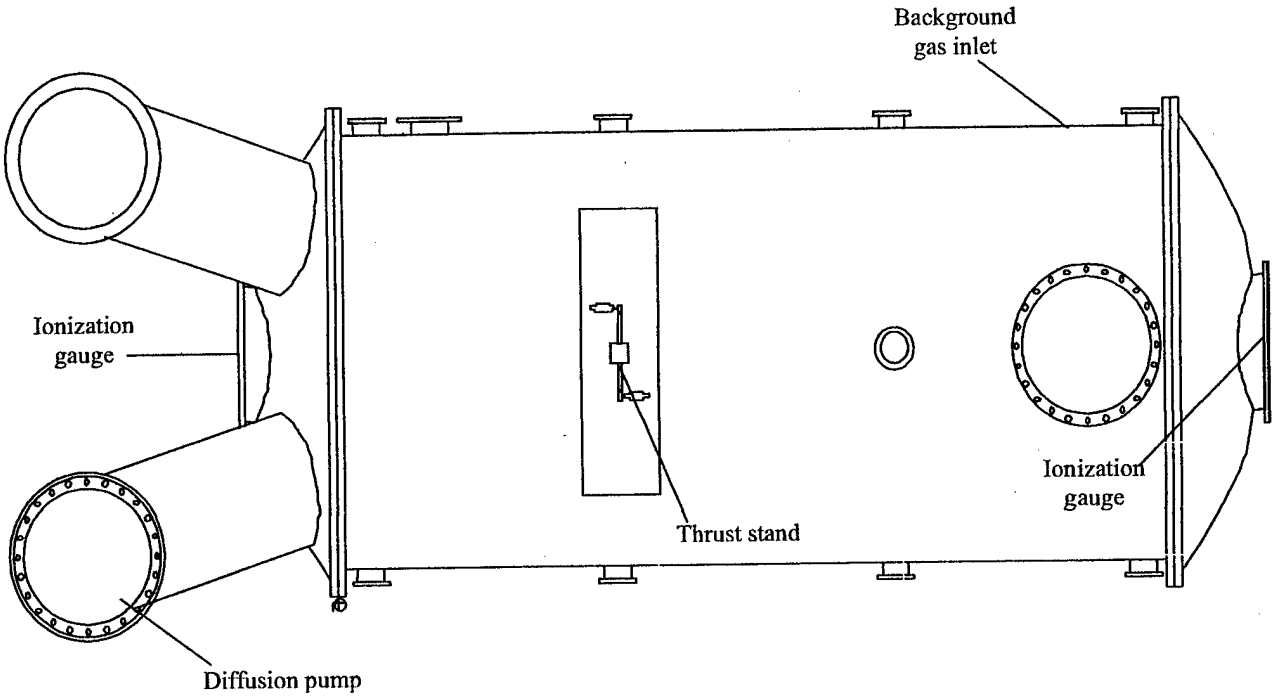

Figure 5 Jamison

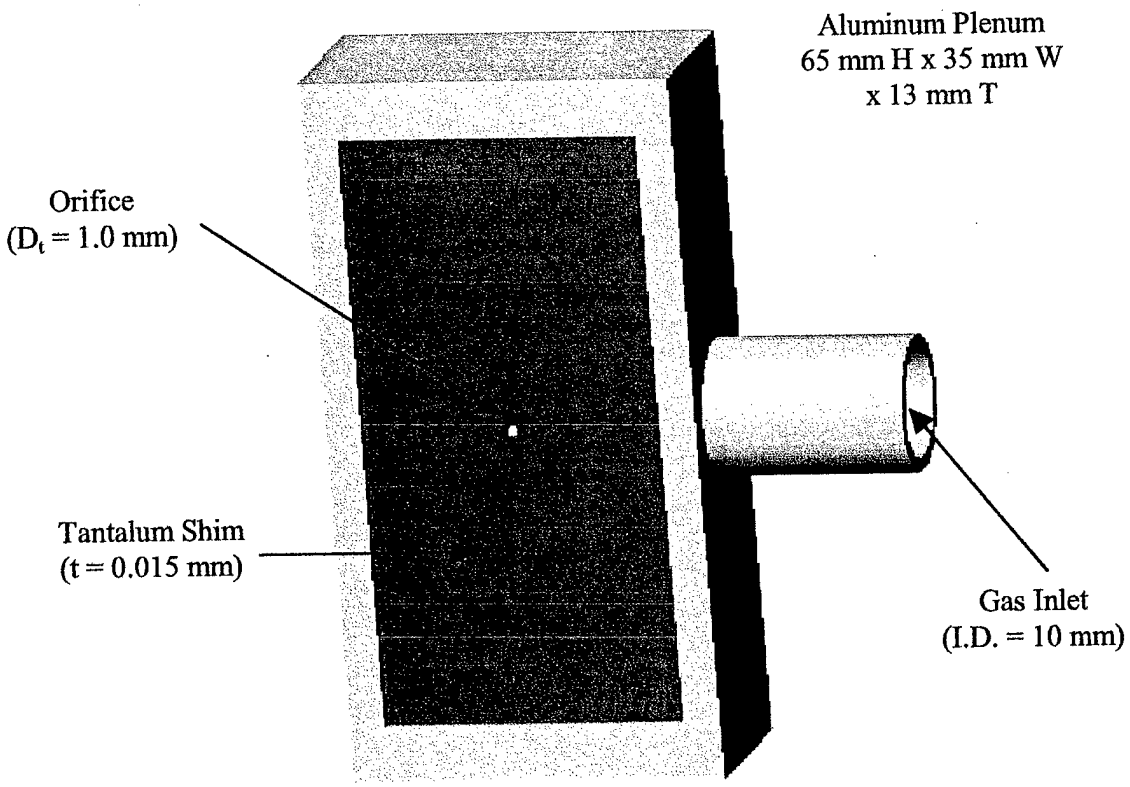

Figure 6 Jamison

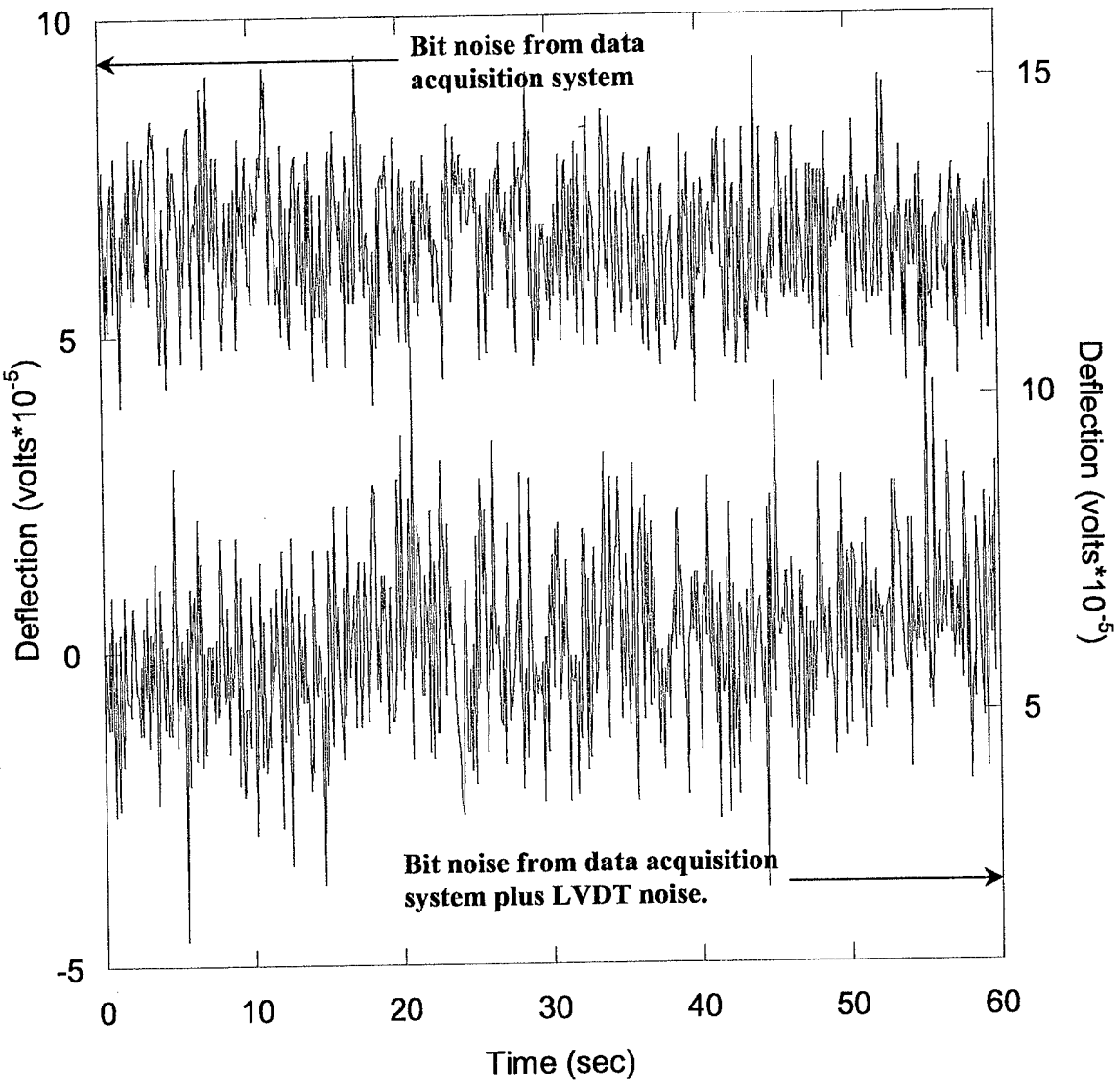

Figure 7 Jamison

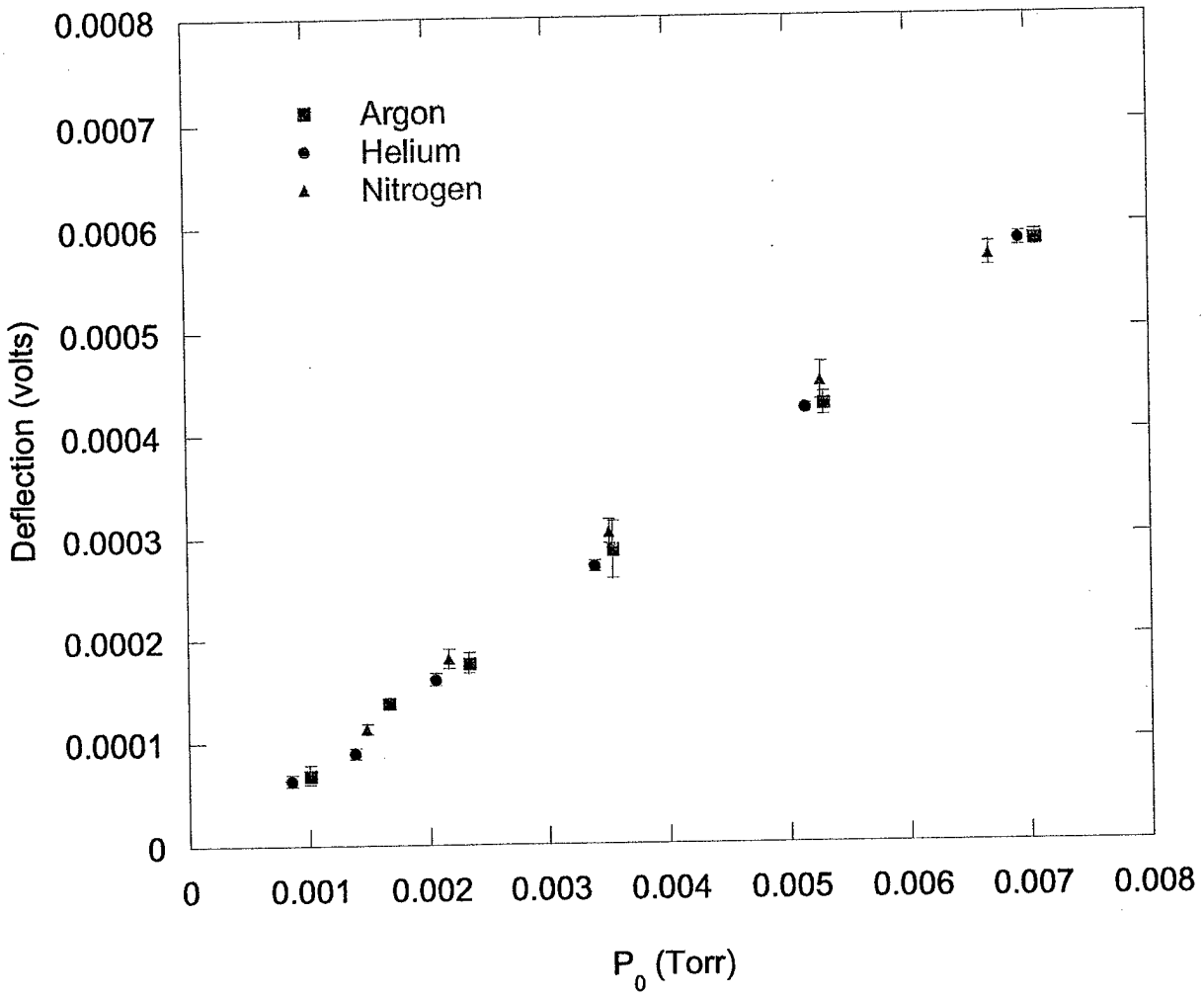

Figure 8 Jamison

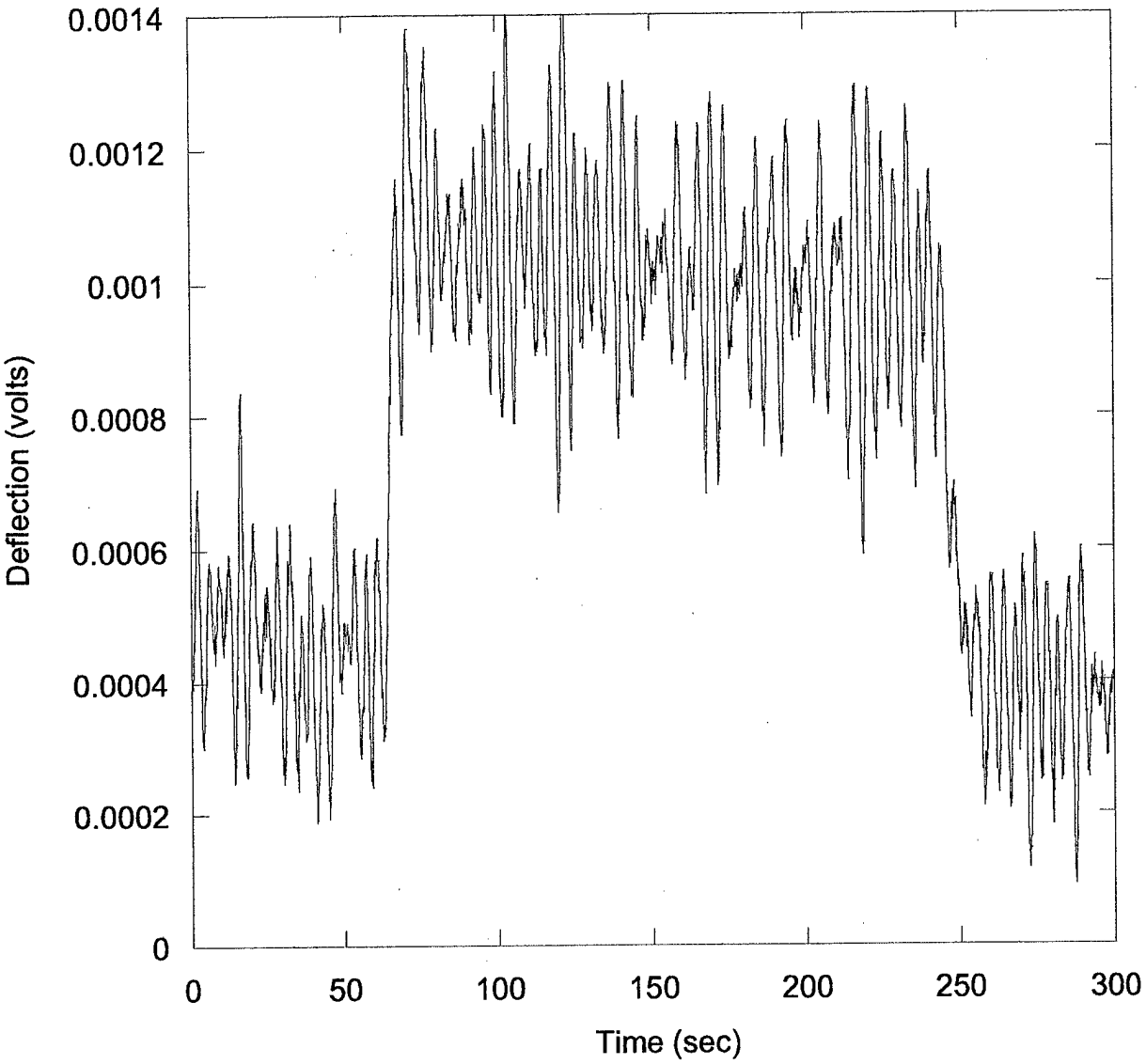

Figure 9a Jamison

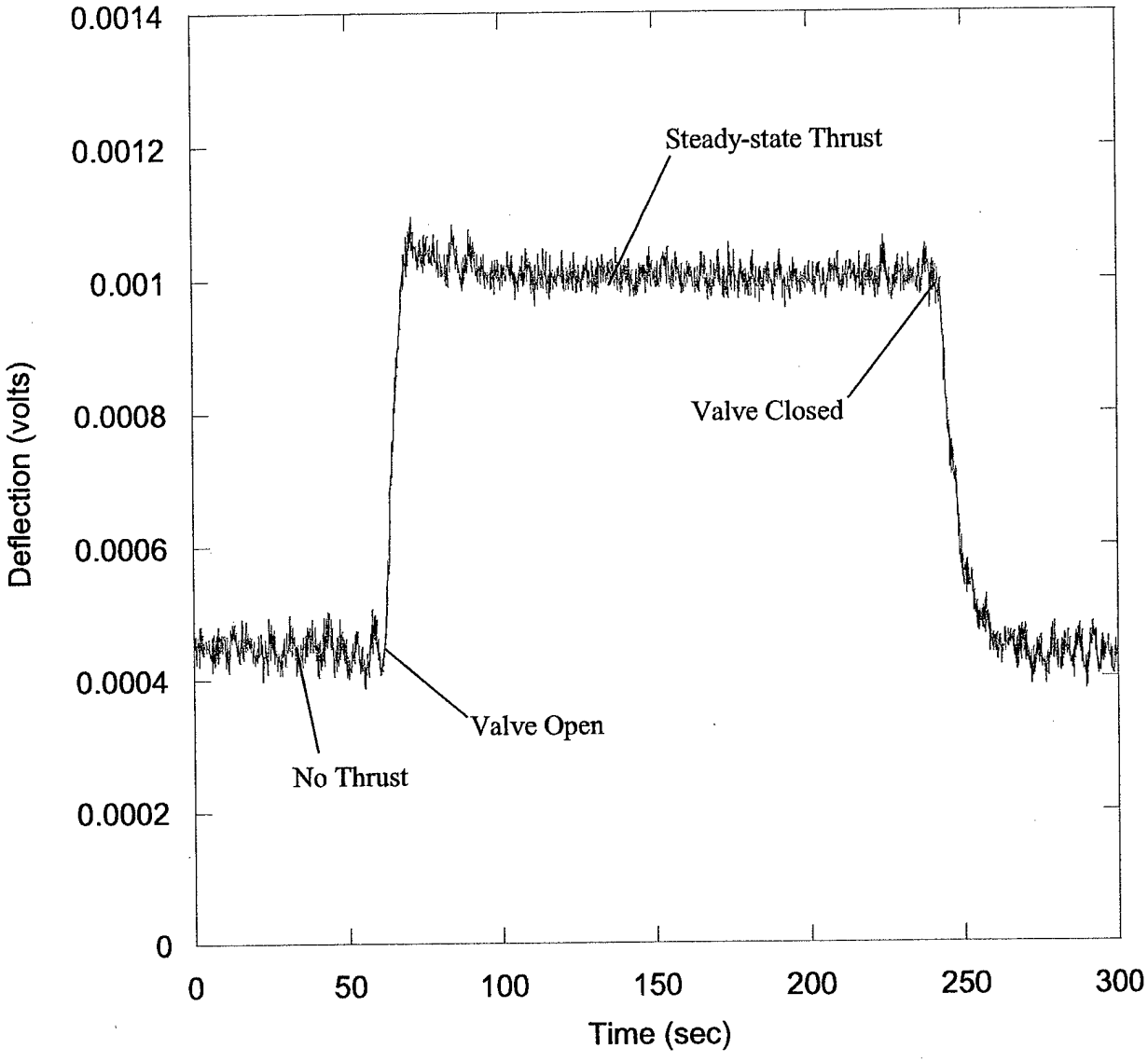

Figure 9b Jamison

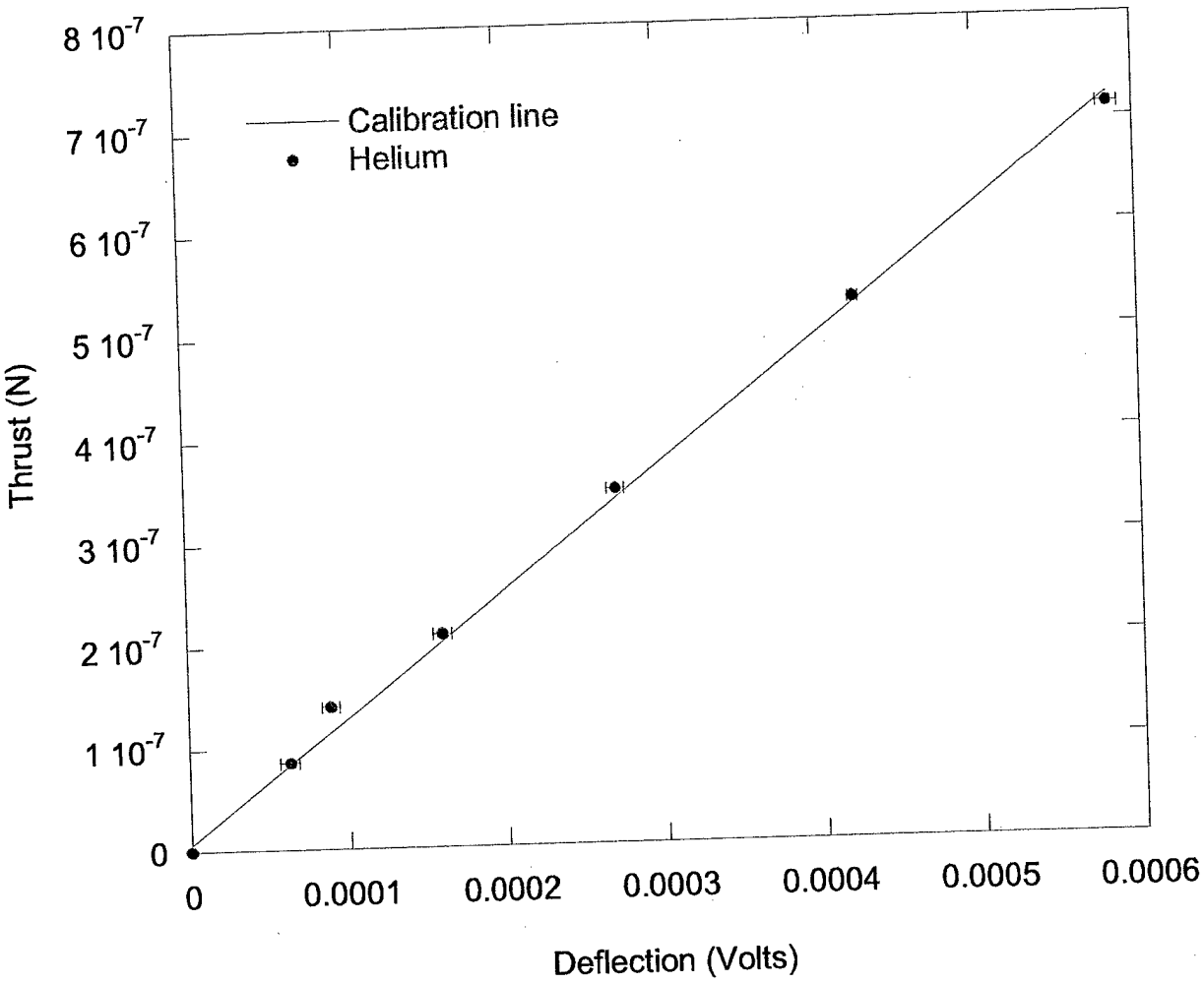

Figure 10 Jamison

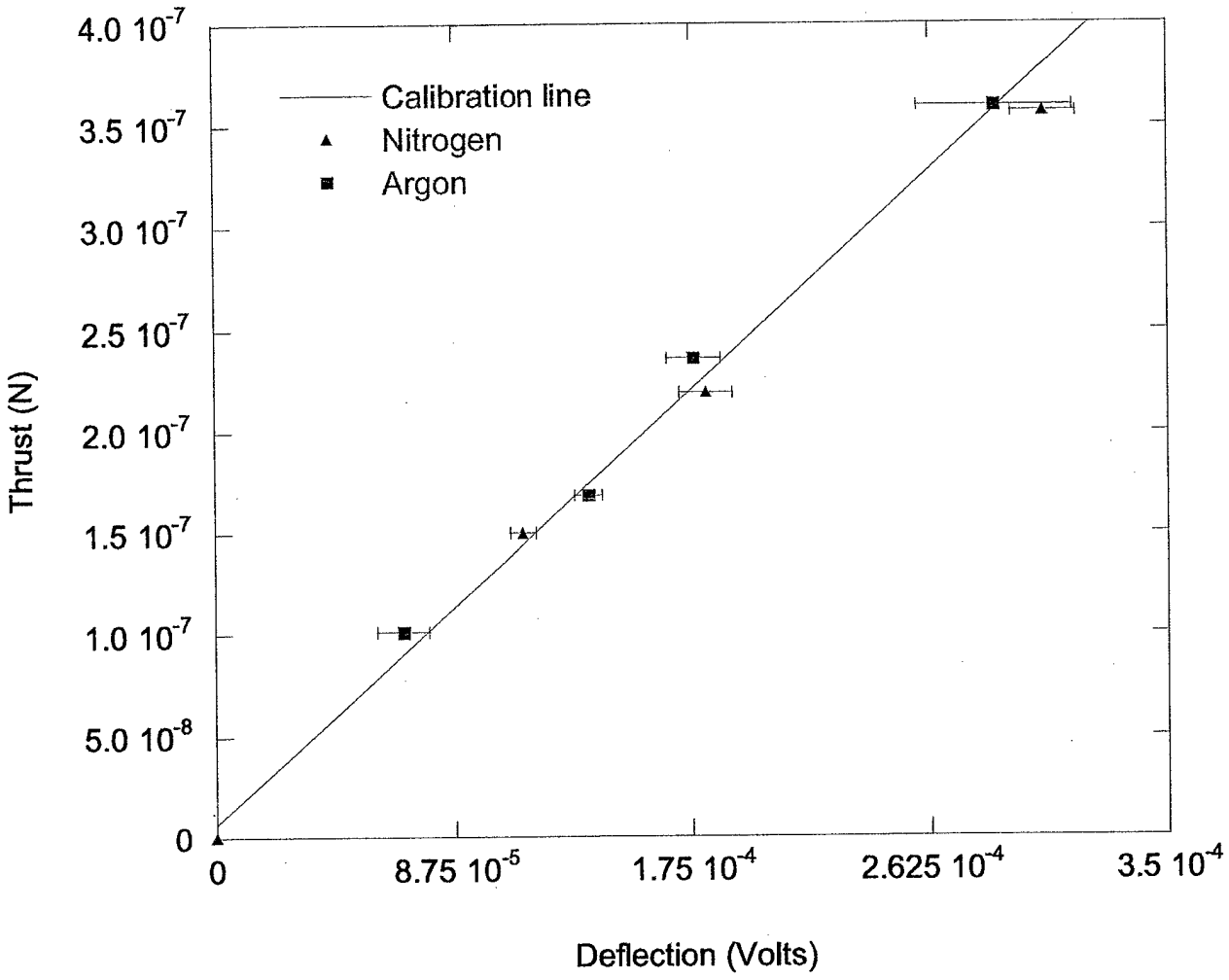

Figure 11 Jamison

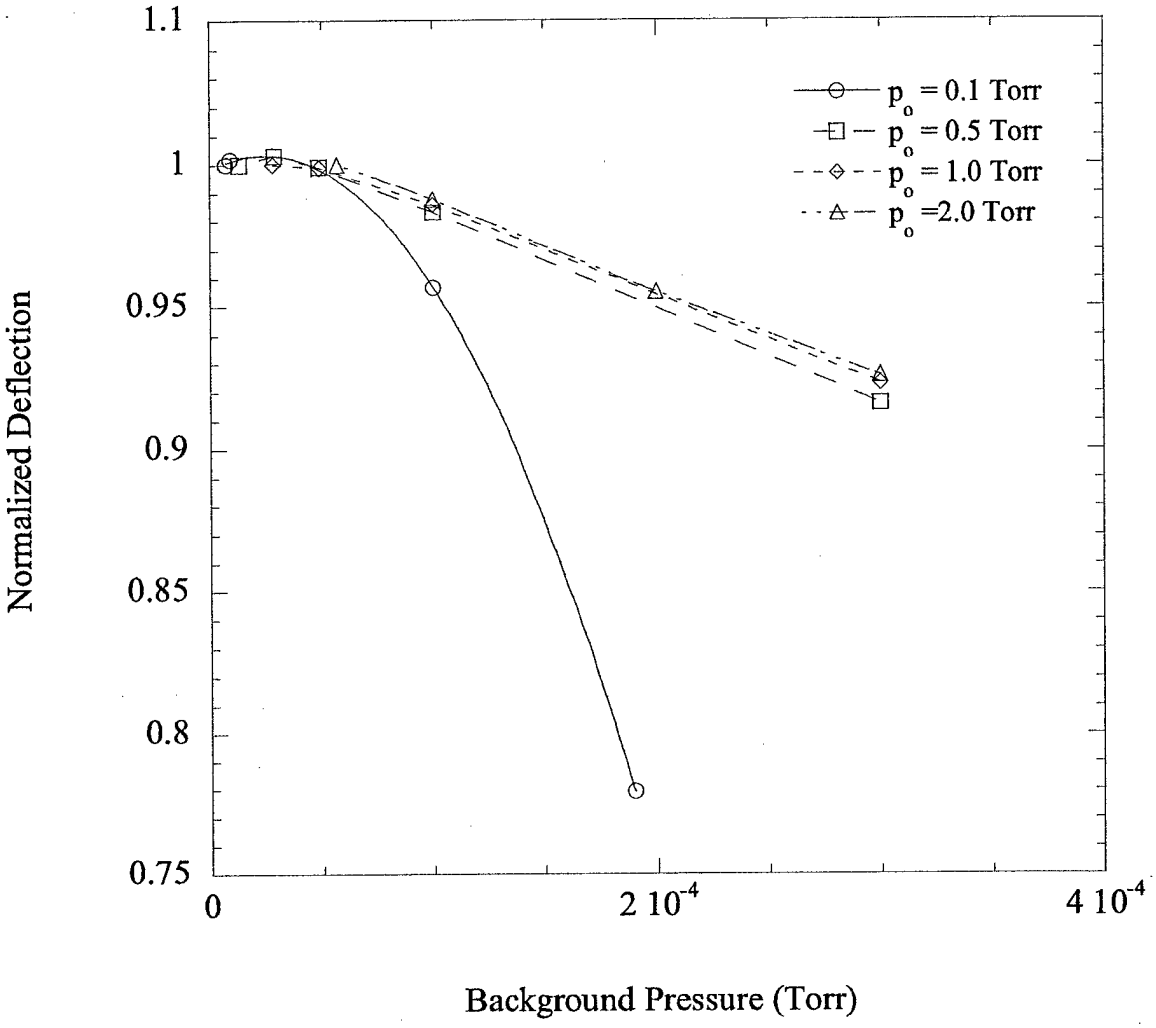

Figure 12 Jamison